NOAA Technical Memorandum NMFS-AFSC-471

Distribution and Estimated Abundance of Eastern Bering Sea Belugas from Aerial Line-Transect Surveys in 2017

M. C. Ferguson, A. A. Brower, A. L. Willoughby, and C. L. Sims

July 2023

U.S. DEPARTMENT OF COMMERCE

National Oceanic and Atmospheric Administration
National Marine Fisheries Service
Alaska Fisheries Science Center

The National Marine Fisheries Service's Alaska Fisheries Science Center uses the NOAA Technical Memorandum series to issue informal scientific and technical publications when complete formal review and editorial processing are not appropriate or feasible. Documents within this series reflect sound professional work and may be referenced in the formal scientific and technical literature.

The NMFS-AFSC Technical Memorandum series of the Alaska Fisheries Science Center continues the NMFS-F/NWC series established in 1970 by the Northwest Fisheries Center. The NMFS-NWFSC series is currently used by the Northwest Fisheries Science Center.

This document should be cited as follows:

Ferguson, M. C., Brower, A. A., Willoughby, A. L., and Sims, C. K. 2023. Distribution and estimated abundance of eastern Bering Sea belugas from aerial line-transect surveys in 2017. U.S. Dep. Commer., NOAA Tech. Memo. NMFS-AFSC-471, 50 p.

This document is available online at:

Document available: https://repository.library.noaa.gov

NOAA FISHERIES

Distribution and Estimated Abundance of Eastern Bering Sea Belugas from Aerial Line-Transect Surveys in 2017

M. C. Ferguson[1], A. A. Brower[1,2], A. L. Willoughby[1,2], and C. L. Sims[1,2]

[1]Marine Mammal Laboratory
Alaska Fisheries Science Center
National Marine Fisheries Service
National Oceanic and Atmospheric Administration
7600 Sand Point Way NE
Seattle, WA 98115

[2]Cooperative Institute for Climate, Ocean, and Ecosystem Studies
University of Washington
Seattle, WA 98105

U.S. DEPARTMENT OF COMMERCE

National Oceanic and Atmospheric Administration
National Marine Fisheries Service
Alaska Fisheries Science Center

NOAA Technical Memorandum NOAA-TM-AFSC-471

July 2023

ABSTRACT

The Eastern Bering Sea (EBS) beluga (*Delphinapterus leucas*) stock inhabits the waters of Norton Sound and the Yukon River Delta, Alaska, during the ice-free period from spring sea ice breakup to autumn freeze-up. During June, July, and August, belugas aggregate near the Yukon River Delta, where they feed on seasonally abundant salmon (*Oncorhynchus* spp.). EBS belugas are an important nutritional and cultural resource to Alaska Natives, and are harvested by more than 20 communities in Norton Sound and the Yukon. To collect data for an updated abundance estimate for EBS belugas, aerial line-transect surveys were conducted in Norton Sound and off the Yukon River Delta from 16 through 29 June 2017. During the 14-day survey period, 16 survey flights were conducted on 12 days, covering more than 8,500 km of transect effort. Throughout the study area, 741 beluga groups totaling 1,897 belugas were sighted. Similar to previous aerial surveys, the highest densities of belugas extended approximately 25 km offshore along the Yukon River Delta to the west of Pastol Bay, broadening to approximately 120 km offshore northward to Unalakleet. The first step in estimating abundance was a geographically stratified, multiple covariates distance sampling analysis that examined the effects of group size, turbidity, Beaufort Sea State, and perpendicular sighting distance on detection probability. The resulting abundance estimate for the EBS beluga stock, prior to correcting for belugas within the observers' field of view but below the water's surface and unable to be detected (availability bias) and for belugas at the surface near the transect but not detected (transect detection probability), was 4,621 belugas (CV = 0.116; 95% CI [3,635-5,873]). We estimated the correction factor for availability bias to be 2.0 based on historical beluga surface and dive interval data and an estimate of the viewing time for a marine mammal observer during the 2017 aerial survey. Data were not collected during the 2017 aerial survey to estimate a transect

detection correction factor specific to the survey. Therefore, transect detection probability was estimated from imagery and marine mammal observer data collected during similar aerial line-transect surveys for marine mammals in the eastern Chukchi and western Beaufort seas during 2018 and 2019. To accommodate uncertainty in matching belugas detected in the imagery with belugas detected by the aerial marine mammal observers, a sensitivity analysis was conducted that considered three different assumptions critical to the matching process. The sensitivity analysis resulted in three estimates of transect detection probability ranging from 0.648 to 0.785, which produced three estimates of EBS beluga abundance (and associated uncertainty) in 2017 that ranged from 11,768 (CV = 0.117) to 14,243 (CV = 0.231) belugas. We used expert judgment to select a single best estimate of transect detection probability. Given the transect detection probability estimate that the experts believed to be most appropriate, the resulting abundance estimate for EBS belugas in 2017 was 12,269 belugas (CV = 0.118).

CONTENTS

INTRODUCTION

Belugas (*Delphinapterus leucas*) from the Eastern Bering Sea (EBS) stock are an important nutritional and cultural resource for Indigenous communities near Norton Sound and the Yukon River Delta. These areas are experiencing rapid ecological changes and increased human activities. EBS belugas are one of four beluga stocks that have been co-managed since 1988 by the Alaska Beluga Whale Committee (ABWC, which includes hunters, resource managers, and scientists) and NOAA's National Marine Fisheries Service (NOAA Fisheries; Adams et al. 1993, Frost and Suydam 2021).

The distribution and movement patterns of EBS belugas are primarily known from Indigenous and other local knowledge (Huntington et al. 1999, Oceana and Kawerak, Inc. 2014, Lowry et al. 2017), aerial surveys (Lowry et al. 2017), telemetry studies (Citta et al. 2017), and genetics (e.g., O'Corry-Crowe et al. 2018, 2021). EBS belugas predictably occur in the Norton Sound/Yukon Delta region during the period from shortly after sea ice breakup (usually mid-May) until freeze-up (usually November) (Lowry et al. 2017, Citta et al. 2017). Belugas from this stock are harvested at more than 20 villages during spring, summer, and autumn (Lowry et al. 2019). Their distribution from spring through autumn reflects high densities of prey, particularly fishes (Lowry et al. 2017), and also may be affected by sea ice conditions and human disturbance (Huntington et al. 1999, Oceana and Kawerak Inc. 2014). During the rest of the year (December through April), two of the three belugas from this stock that were tagged with satellite transmitters remained in the Bering Sea, but their range shifted south towards Bristol Bay and west to the offshore waters of the Bering Sea (Citta et al. 2017). The third tagged EBS beluga traveled north into the southern Chukchi Sea in November-December before returning back south into the Bering Sea (ABWC unpublished data).

To evaluate the sustainability of beluga subsistence harvests, ABWC estimated EBS beluga abundance using aerial surveys in Norton Sound and along the Yukon River Delta each year from 1992 to 1995 and 1999 to 2000 (Lowry et al. 2017). In 1992, aerial surveys were conducted in May, June, and September to determine the best month for conducting future surveys. Based on those results, aerial surveys for all remaining years were conducted in June, when belugas tend to concentrate near Pastol Bay and the Yukon River Delta. Lowry et al. (2017) derived an estimate of abundance for the EBS beluga stock from the aerial surveys conducted in June 2000. During the 2000 survey, belugas were rarely sighted in northern Norton Sound, so survey effort was restricted to central and southern Norton Sound and the Yukon River Delta. Based on a geographically stratified distance sampling analysis, the number of belugas estimated to be at the surface in the study area was 3,497 (CV = 0.37). That estimate did not correct for belugas in the study area that were not available to be seen because they were outside of the observers' field of view or too deep in the water column to be seen (availability bias; Marsh and Sinclair 1989), nor did it correct for belugas on the transect that were available to be seen but were not detected (transect detection probability, a component of perception bias; March and Sinclair 1989, Laake and Borchers 2004). Lowry et al.'s (2017) best estimate of stock abundance in 2000 was 6,994 belugas (95% confidence interval 3,162-15,472), incorporating a correction factor of 2.0 to account for availability bias.

During June 2017, ABWC and NOAA Fisheries collaborated to conduct an aerial line-transect survey in Norton Sound and along the Yukon River Delta to update the estimate of abundance for the EBS beluga stock. Confidence in cetacean abundance estimates for decisions related to management and conservation actions decreases with the age of the estimate because abundance

may change over time, and 17 years had passed since the previous aerial surveys were conducted to estimate abundance of EBS belugas. Here, we present the results of the 2017 aerial survey for EBS belugas and an abundance estimate that incorporates correction factors for availability bias and transect detection probability.

METHODS

Study Area

Norton Sound is a shallow bay (average depth 13 m) located along western Alaska, south of the Seward Peninsula, spanning approximately 160 km from Cape Nome to the Yukon River Delta (Fig. 1). The sound is seasonally covered with sea ice. During June, sea ice is usually absent, which was the case in June 2017. Outflow from the Yukon River creates a nearshore zone of turbid water, extending approximately 40 km offshore, bounded by a sharp oceanographic front, beyond which the waters are clearer and it is possible to see below the surface of the water from an aerial platform.

Eastern Bering Sea Beluga Aerial Line-transect Survey Methods

Aerial line-transect surveys were flown in Norton Sound and along the Yukon River Delta, from 15 to 29 June 2017 (Fig. 1). Following Lowry et al. (2017), systematic transects were placed 9.3 km apart, based on a grid with a randomly selected start point. Transect length varied from approximately 20 to 265 km. Transects were oriented east-west, along lines of latitude, from shore to 166° W, extending from the northernmost transect in Norton Bay to the southernmost transect at 62.3° N, approximately 50 km north of Scammon Bay. For consistency with Lowry et al. (2017), the same four survey strata were used in 2017 (Fig. 1). The total study area was 41,416 km^2, and the area of the four strata was 28,946 km^2. Each transect was surveyed at least once over the course of the 2-week field season.

The Turbo Commander aircraft provided and flown by Clearwater Air, Inc., was based in Nome, Alaska. Unalakleet, Alaska, was an alternate airport that was used for refueling when conducting surveys of the central and southern transects. The Turbo Commander is a twin-turbine, high-wing aircraft. The plane had bubble windows for the left- and right-side primary observers, allowing unobstructed views from directly beneath the plane out to the horizon. Surveys were conducted at 320 m altitude and 213 km/h speed.

The survey team comprised two primary observers and one dedicated data recorder. All three observers had considerable previous experience (8.5-13 years, mean 10.7 years) conducting aerial line-transect surveys for cetaceans. The observers' marine mammal aerial survey experience in Alaska ranged from 3 to 13 years (mean = median = 8 years).

The data recorder input sighting data into a laptop computer, connected to a GPS, running specialized, menu-driven software (Clarke et al. 2020; MML unpublished report). Time and position data (latitude, longitude, altitude) were automatically recorded in 30-sec intervals or whenever a manual data entry was recorded. Environmental and viewing conditions, including integer-valued Beaufort Sea State, turbidity (binary, yes or no), visibility range perpendicular to the aircraft on each side of the plane (< 1 km, 1-2 km, 2-3 km, 3-5 km, 5-10 km, or unlimited), sky conditions (clear, partly cloudy, overcast), integer-valued sea ice percent (the average from both sides of the plane), and impediments to visibility (glare, fog, haze, precipitation, ice on the window, low ceiling) on each side of the plane were recorded in 5-min intervals or whenever conditions changed.

Primary observers scanned with the naked eye, using binoculars only to check potential targets or get a magnified view on a confirmed target. Declination angles from the horizon to each sighting were measured using handheld clinometers when the sighting was abeam. One

"sighting" or "group" was defined as all animals within 5 body lengths of each other. Therefore, a group could comprise one or more animals. Belugas in the study area during June are typically distributed in small groups comprising only a few animals. Therefore, survey effort was largely conducted in passing mode, breaking off transect to circle sightings only in exceptional situations (e.g., to photograph carcasses or investigate sightings of cetaceans that were not belugas to confirm species identification). Sightings that could not be positively identified to species were recorded at the taxonomic level to which they could be identified (e.g., unidentified cetacean or small unidentified pinniped). If group size could not be determined with confidence, high and low estimates could also be recorded. Beluga calves were identified primarily based on size: calves were noticeably smaller than the other animals. In addition to being smaller, coloration (typically grayish or brownish pigmentation) and close proximity to an adult helped observers identify beluga calves. However, it is not always possible for aerial observers to distinguish beluga calves of the year from juveniles; therefore, animals recorded as beluga calves likely include belugas up to a few years old. The observers watched for any abrupt and unexpected changes in the whales' initially observed behavior, presumably due to the aircraft. Observed responses and the number of whales that responded were recorded in the database.

Four survey modes were used for data collection: deadhead, transect, circling from transect, and search. Deadhead effort occurred during transit or when weather was not conducive to surveying; no sighting data were collected during deadhead. During the remaining three survey modes, observers were actively surveying and all sightings and environmental data were recorded. Transect effort refers to systematic survey effort along a prescribed transect line. Search refers to non-systematic survey effort during transit or between transects. Circling from transect occurred

when the aircraft diverted from flat and level flight to circle a localized area to investigate a sighting or potential sightings.

ASAMM Imagery Collection and Analysis Methods

During the 2017 EBS beluga surveys, data were not collected to estimate transect detection probability. Therefore, we relied on the best information available to us from data from the Aerial Surveys of Marine Mammals (ASAMM) line-transect surveys conducted in the eastern Chukchi and western Beaufort seas from July through October in 2018 and 2019 (Clarke et al. 2019, 2020). These surveys targeted belugas and larger cetaceans; marine mammal observer and imagery data were collected concurrently. ASAMM line-transect survey protocols were comparable to those used during the 2017 EBS beluga aerial survey and are detailed in Clarke et al. (2019, 2020). Additionally, the same aircraft (including bubble windows) and marine mammal observer configuration used during the 2017 EBS beluga aerial survey were also used to conduct the ASAMM flights that collected the data we describe below. ASAMM surveys were flown at the same target speed (213 km/h speed) and a similar target altitude (400 m) as the 2017 beluga surveys (320 m). Beluga group size distributions were comparable in the 2017 EBS beluga data and the relevant ASAMM survey data. For the 2017 EBS beluga survey, 54.7% (338/618) of the sightings were of single belugas, 23.6% (146/618) comprised two belugas, 21.4% (132/618) had 3-10 belugas, and < 1% (2/618) had more than 10 belugas. In the 2018-2019 ASAMM survey data, 70.9% (720/1015) of the sightings were of single belugas, 17.1% (174/1015) comprised two belugas, 10.6% (108/1015) had 3-10 belugas, and 1.3% (13/1015) had more than 10 belugas. Therefore, we believe the estimates of transect detection probability from ASAMM provide reasonable approximations to the actual value for the 2017 EBS beluga aerial surveys.

To estimate transect detection probability for marine mammal observers (i.e., aerial observers) on the ASAMM project, a downward-pointing digital single lens reflex camera with a 20- or 21-mm lens mounted to the belly of the aircraft collected true color (red, green, and blue [RGB]) imagery (Clarke et al. 2019, 2020). At 400 m survey altitude, a single image taken with the 21-mm lens captured a parcel of water measuring approximately 684 m perpendicular to the transect (342 m on each side of the transect) and 457 m along the transect. One image was collected every 2 to 3 seconds, resulting in each parcel of water being visible in three to four images. The imagery served as an "independent observer" for a mark-recapture analysis of the ASAMM aerial observer data.

Willoughby et al. (2021) provide detailed imagery collection and analysis methods and results; here, we present a brief overview. Metadata automatically written to each image included latitude, longitude, date, and time. Every third image collected was manually reviewed post-flight for marine mammal sightings by trained photo analysts. All sightings detected in the imagery were manually compared to the aerial observer database to determine matches based on date, time, and location (side of plane and distance from transect). The results of the matching analysis could be one of three categories: matched, not-matched, and "inconclusive results" (abbreviated "IR"). Inconclusive results meant that the photo analyst could not determine for certain whether an imagery sighting was also detected by the aerial observers. Although Willoughby et al. (2021) did conduct the complementary analysis to determine which sightings in the aerial observer database were also detected in the imagery, we do not present those results here because we were only concerned with the detection probability of the aerial observers, not the aptitude of the imagery and photo analysts.

Analytical Methods

All analyses were conducted in R Statistical Software (v. 4.0.5; R Core Team 2021) with packages maptools (Bivand and Lewin-Koh 2019), mgcv (Wood 2017), mrds (Laake et al. 2021), sp (Pebesma and Bivand 2005, Bivand et al. 2013), rgdal (Bivand et al. 2019), and rgeos (Bivand and Rundel 2019). All geospatial data were projected into an Equidistant Conic projection (false easting: 0.0; false northing: 0.0; central meridian: -164.0°; latitude of origin: 63.5°; standard parallels: 62.5°, 64.5°; linear unit: meter [1.0]; WGS84 datum). All analyses in this paper were limited to data collected during conditions of Beaufort Sea State 4 or less.

The basic line-transect estimator of animal density is (Buckland et al. 2001, Burt et al. 2014):

$$\widehat{D} = \frac{1}{a}\sum_{j=1}^{n_g}\frac{S_j}{\widehat{p_1}\left(\hat{\theta}; \boldsymbol{z}_j\right)} \quad [1]$$

where

n_g = total number of groups detected;

S_j = size of group indexed by j;

a = area searched, which is equal to $2wL$;

L = total length of transects surveyed;

w = width of the strip searched on one side of the aircraft; and

$\widehat{p_1}\left(\hat{\theta}; \boldsymbol{z}_j\right)$ = estimate of the overall probability that an aerial observer detects group j, given covariates $\boldsymbol{z}_j$ that affect detectability.

The probability that an aerial observer ("observer 1") detects a group (indexed by *j*) of visible belugas located on the transect and the effects of distance (y) from the transect (and possibly other covariates $\boldsymbol{z_j}$) on detection probability were estimated using an observation model, denoted

by $p_1(y, \boldsymbol{z_j})$. The underlying observation model for the EBS beluga aerial survey was a scaled version of a multiple covariates distance sampling (mcds) detection function, $g(y, \boldsymbol{z_j})$, (Marques and Buckland 2003, Laake and Borchers 2004):

$$p_1(y, \boldsymbol{z_j}) = p_1(0, \boldsymbol{z_j}) g(y, \boldsymbol{z_j}). \quad [2]$$

The mcds detection function assumes the probability of detecting an object on the transect equals 1.0; it specifies the functional form (shape and scale) of the observation model. The scaling factor in the observation model is the mark-recapture component, $p_1(0, \boldsymbol{z_j})$, which determines the location of the intercept in the observation model and represents the probability that an aerial observer detects an object located on the transect (or the left-truncation point), at $y = 0$. Because belly port imagery were collected only during surveys conducted in the ASAMM study area in 2018 and 2019, the estimate of transect detection probability, $p_1(0, \boldsymbol{z_j})$, from ASAMM was incorporated into the observation model for the EBS beluga aerial survey. We first present the analytical methods used to construct the mcds detection function, followed by those for the mark-recapture model.

Multiple Covariates Distance Sampling Detection Function for the EBS Beluga Aerial Survey

The mcds detection function was constructed using data only from the 2017 EBS beluga aerial survey, which were filtered prior to fitting the model. Only beluga sightings made by primary observers during transect effort that had recorded declination angles were used to construct the detection function.

Additionally, sighting data were truncated close to and far from the transect. Data were left-truncated to account for lower sighting probabilities very close to the aircraft (Hain et al. 1999). The histogram of perpendicular distances to beluga sightings indicated fewer than expected

sightings within 50 m of the transect; therefore, the data were left-truncated at 50 m (Fig. 2). The farthest 5% of sightings were omitted from the detection function analyses to minimize the effects of outliers; this right-truncation distance was 944 m and corresponds to *w*, the width of the strip searched on one side of the aircraft.

A mcds model can take various forms, specified by its key function, such as the half-normal key function or hazard-rate key function. For the EBS beluga aerial survey, mcds detection function models with half-normal and hazard-rate key functions were considered. A half-normal model in which the standard deviation (scale parameter) is a linear function of covariates affecting detection probability may be represented as:

$$g(y, \boldsymbol{z_j}) = exp\left(\frac{-y^2}{2\left[exp\{\theta_0 + \sum_j \theta_j z_j\}\right]^2}\right) \quad [3]$$

An analogous hazard-rate model may be represented as:

$$g(y, \boldsymbol{z_j}) = 1 - exp\left[-\left(\frac{y}{exp\{\theta_0 + \sum_j \theta_j z_j\}}\right)^{-b}\right] \quad [4]$$

The null hazard-rate models had considerably lower AIC values and exhibited better fit (based on visual inspection of the detection function curve overlaid on the histogram of perpendicular sighting distances) than the half-normal models, so covariate selection proceeded with only the hazard-rate key function. The average probability that an aerial observer detects an object that is available to be seen, given covariates $\boldsymbol{z_j}$ that affect detectability, assuming transect detection probability is 1.0, is:

$$p^*(\boldsymbol{z_j}) = \frac{\int_0^w g\,(y, \boldsymbol{z_j}) dy}{w} \quad [5]$$

The potential covariates considered for inclusion in the mcds detection function were four different group size variables, turbidity, and Beaufort Sea State (Table 1). Forward stepwise selection of covariates, based on AIC, was used to choose a single best mcds detection function

model. Although four different group size covariates were considered in the initial univariate model, only the covariate with the lowest AIC value among the univariate group size models was retained for further consideration in the model fitting and selection process.

Some transect lines were flown on multiple days over the course of the 2017 field season. Therefore, transect ID was used as the analytical sample unit for estimating abundance within each of the four geographic strata. Sightings and effort from multiple flights down a single transect on multiple days were pooled so that the sum of all sightings and the sum of all effort associated with the transect were used to estimate encounter rate variance via the R2 estimator (Fewster et al. 2009).

Mark-recapture Detection Functions for ASAMM

To derive transect detection probability for an aerial observer, $p_1(0, \boldsymbol{z_j})$, a mark-recapture detection function model was constructed. The mark-recapture model was constructed from belly port imagery and aerial line-transect observer sightings and effort data collected during ASAMM surveys conducted in the eastern Chukchi and western Beaufort seas between July and October 2018-2019 (Clarke et al. 2019, 2020).

ASAMM aerial observer data and belly port imagery were filtered prior to building the mark-recapture model. Here, we define the filters for the ASAMM aerial observer data. ASAMM data were limited to flights conducted in 2018 and 2019 when the belly port camera collected imagery. Only beluga sightings made by primary observers during transect or search effort that had recorded declination angles were used to construct the detection function. The histogram of perpendicular distances to beluga sightings indicated fewer than expected sightings within 100 m of the transect; therefore, the data were left-truncated at 100 m (Fig. 3). The farthest 5% of

sightings were omitted from the detection function analyses to minimize the effects of outliers; this right-truncation distance was 1,141 m.

Imagery sighting filters were consistent with those for the ASAMM aerial observer data. Only images taken during straight and level flight, when the aerial observers were actively searching for cetaceans and when low clouds or precipitation obscured less than 50% of the frame were analyzed. ASAMM and EBS beluga aerial line-transect surveys were typically not conducted, or effort was aborted, during conditions with extensive low clouds or precipitation because those impediments to visibility negatively affect the aerial observers' ability to detect cetaceans. The perpendicular distance from the transect to each imagery sighting was calculated based on the following variables: location of the sighting along the horizontal axis of the image (measured in pixels); camera sensor dimensions (in pixels); focal length of the lens; and survey altitude, which was taken as the altitude corresponding to the closest record in the ASAMM database. Imagery sightings located on either side of the transect within the left-truncation distance of the ASAMM data (100 m) were excluded from the mark-recapture detection function model. If the same group of belugas was detected in more than one image, only a single detection was included in the model; duplicate detections were omitted.

In a sensitivity analysis, we considered four methods to analyze the IR sightings (imagery sightings that were not known for certain to be matched or missed by the aerial observers). First, we examined the feasibility of applying the methods of Hamilton et al. (2018), which involve a threshold-free probabilistic approach to identify matches and estimate group size. However, we found that our data were not conducive to their approach. Specifically, using a slight modification of Hamilton et al.'s (2018) method that we tailored to our data, approximately 15-20% of the imagery sightings that photo analysts classified as having certain matches in the

ASAMM database were subsequently classified as being unmatched by the matching algorithm; in contrast, approximately 3-5% of the imagery sightings that photo analysts classified as being missed by the aerial observers were subsequently classified as being matched by the algorithm. Second, we assumed that all IR sightings were detected by the aerial observers; we refer to this as the IR-detected scenario. Third, we assumed that all IR sightings were missed by the aerial observers; we refer to this as the IR-missed scenario. Lastly, for the IR-omitted scenario, we omitted all IR sightings from the analysis, but kept all other ASAMM observer data and imagery in the analysis the same.

We used expert judgment to select a single estimate of transect detection probability to derive the recommended estimate of abundance of EBS belugas in 2017. Expert judgment is a common tool used in conservation science and natural resource management (e.g., Danovaro et al. 2020, Lettrich et al. 2020), disciplines in which decisions often need to be made even when information is limited.

Fundamentally, a basic mark-recapture detection function model can estimate the probability that an aerial observer detects an object that the photo analyst ("observer 2") detected, $p_{1|2}(y, \boldsymbol{z_j})$. Our model for $p_{1|2}(y, \boldsymbol{z_j})$ was based on trial configuration of observers, with the assumption of point independence (Laake and Borchers 2004). Trial configuration is appropriate here because imagery were used to estimate transect detection probability for the aerial observers; there was no need to derive a detection function for the photo analysts. Point independence requires that detections of objects located on the transect are independent between the aerial observers and photo analysts, but not necessarily elsewhere. Due to the assumption of point independence, $p_1(0, \boldsymbol{z_j}) = p_{1|2}(0, \boldsymbol{z_j})$.

Mark-recapture estimators are inherently plagued by bias due to unmodeled heterogeneity in detection probability, and distance is one of the largest sources of detection probability heterogeneity in distance-sampling data (Laake and Borchers 2004). The model for $p_{1|2}(y, \boldsymbol{z_j})$ allows detection probability to depend on perpendicular distance from the aircraft and other covariates. The additional covariates considered for inclusion in the mark-recapture model were related to Beaufort Sea State and group size (Table 2). The ASAMM study area does not include turbid habitats like the waters off the Yukon River; therefore, the effects of turbidity on transect detection probability could not be examined in the present analysis. The logistic model was used for the mark-recapture detection function (Laake and Borchers 2004):

$$p_{1|2}(y, \boldsymbol{z_j}) = \frac{exp\{\beta_0 + \beta_y y + \sum_j \beta_j z_j\}}{1 + exp\{\beta_0 + \beta_y y + \sum_j \beta_j z_j\}} \quad [6]$$

Transect detection probability for the ASAMM aerial observers in 2018 and 2019, averaged over all $\boldsymbol{z_j}$, was estimated by (Laake and Borchers 2004):

$$\hat{p}_1(0) = \frac{\sum_j^{n_1} \hat{p}_1(0, \boldsymbol{z}_j)/\widehat{\mathbb{E}}\left(\hat{p}_1(\boldsymbol{z}_j)\right)}{\sum_j^{n_1} 1/\widehat{\mathbb{E}}\left(\hat{p}_1(\boldsymbol{z}_j)\right)} \quad [7]$$

where n_1 = number of groups detected by the ASAMM observers.

A single best mark-recapture model for the IR-detected scenario was selected based on AIC. If a model with fewer covariates was within two AIC units of the model with the lowest AIC, the simpler model was chosen as the final model. The covariates incorporated into the selected mark-recapture model for the IR-detected scenario were used to build the mark-recapture models for the IR-missed and IR-omitted scenarios.

Availability Probability

The inverse of the availability bias correction factor is availability probability, p_a. Availability probability is the probability that a group is at the surface within an observer's field of view (Marsh and Sinclair 1989). Availability probability is a function of the animals' respiratory patterns and the duration of time in which the ocean at perpendicular distance y is in the observer's view (i.e., viewing time). McLaren's (1971) availability probability estimator is:

$$p_a(y) = \frac{s + T(y)}{s + d} \quad [8]$$

where:

s = surface interval duration;

$T(y)$ = duration of time in which the ocean at perpendicular distance y is in the observer's view; this parameter is a function of the observer's field of view; and

d = dive interval duration.

We assumed that the effect of distance on detectability was captured by the mcds detection function model. Therefore, we computed availability probability on the transect, $p_a(0)$, effectively scaling the transect detection probability. Because the field of view from the windows in the Turbo Commander was unobstructed ahead of the plane at the left-truncation distance (Ferguson et al. 2021), $T(0)$ was assumed to be a function of the distance at which a beluga can be detected. Therefore, $T(0)$ for the Turbo Commander was computed by dividing the right-truncation distance (944 m) used to build the mcds detection function model by the survey speed (213 km/h). The resulting estimate of viewing time for the Turbo Commander was 15.9 sec.

The best available information on beluga respiration patterns was from behavioral observations made on three adult female belugas tagged with VHF radio tags: one beluga tagged in Bristol Bay, Alaska, in June 1983, and two belugas tagged in Cunningham Inlet, Somerset Island, Canada, in July 1988 (Frost et al. 1985, Frost and Lowry 1995).

Frost and Lowry's (1995) reported availability bias correction factors were not directly applicable to our analysis for two reasons. First, their correction factors assumed that $T(0)$ was at most 10.3 sec. Additionally, the surface and dive data collected during the tagging field studies were not available for our analysis. Therefore, we derived our best estimate of availability probability for the EBS beluga aerial survey in 2017 using the summary statistics (Table 1 in Frost and Lowry 1995) and analytical methods presented in Frost and Lowry (1995) that are detailed below, with our estimate of $T(0)$.

Frost and Lowry (1995) derived their availability probability estimator from McLaren's model [8]. Their estimator, $p^*_{a,k}(0)$ for beluga k, is a weighted average of $p_a(0)$ = 1.0 for dives shorter than $T(0)$ and their associated surfacings, and $p_{a,k}(0)$ as calculated by [8] as a function of the average duration of dives longer than $T(0)$ and the average duration of associated surfacings:

$$p^*_{a,k}(0) = \frac{\left(\sum_{i=1}^{n_{d\leq T(0),k}} s_i + \sum_{i=1}^{n_{d\leq T(0),k}} d_i\right)1.0 + \left(\sum_{i=1}^{n_{d>T(0),k}} s_i + \sum_{i=1}^{n_{d>T(0),k}} d_i\right)p_{a,k}(0)}{\sum_{i=1}^{n_k} s_i + \sum_{i=1}^{n_k} d_i} \quad [9]$$

where n indexes the number of surface-dive cycles. Their final estimate of availability probability was a simple average of the $p^*_{a,k}(0)$ for each of the three belugas:

$$p^*_{a,avg}(0) = \frac{1}{3}\sum_{k=1}^{3} p^*_{a,k}(0) \quad [10]$$

Abundance Estimation

For each scenario in the sensitivity analysis, we estimated the abundance of the EBS beluga stock in 2017 as:

$$\widehat{\mathrm{N}} = \frac{A}{a\hat{p}^{*}_{a,avg}(0)\hat{p}_1(0)} \sum_{j=1}^{n_g} \frac{S_j}{\hat{p}^{*}(\mathbf{z_j})} \quad [11]$$

where A is the total of strata 1 through 4 (28,946 km^2), and the remaining variables are as defined above.

In total, we computed three abundance estimates (and their associated CVs, as detailed below), to evaluate the sensitivity of the abundance estimate to the analytical methods used to accommodate the IR sightings (IR-detected, IR-missed, and IR-omitted).

Uncertainty Estimation

The uncertainty in each abundance estimate in the sensitivity analysis was computed using the delta method and the assumption that the mcds detection function parameter estimates for the EBS beluga aerial surveys were independent from the mark-recapture detection function parameter estimates for the ASAMM surveys. Because there are no estimates of uncertainty for availability probability, this parameter did not contribute to the estimated uncertainty in abundance.

Let $\widetilde{N}$ equal the abundance estimate derived from the mcds model for the EBS beluga aerial surveys and let $\widehat{\mathrm{N}} = \frac{\widetilde{N}}{p_a\hat{p}_1(0)}$, the final abundance estimate for each scenario that incorporates transect detection probability and availability probability. The delta method says that:

$$\widehat{Var}(\hat{N}) = \left(\frac{\partial \hat{N}}{\partial \hat{\theta}_i}\right) V_{\hat{\theta}} \left(\frac{\partial \hat{N}}{\partial \hat{\theta}_i}\right)^T \quad [12]$$

where $\left(\frac{\partial \hat{N}}{\partial \hat{\theta}_i}\right)$ is a row vector with partial derivatives of $\hat{N}$ with respect to $\tilde{N}$ and $\hat{p}_1(0)$, and $\left(\frac{\partial \hat{N}}{\partial \hat{\theta}_i}\right)^T$ is its transpose (a column vector). It follows that:

$$\widehat{Var}(\hat{N}) = \frac{\widehat{Var}(\tilde{N})}{\hat{p}_1(0)^2} + \frac{\tilde{N}^2 Var(\hat{p}_1(0))}{\hat{p}_1(0)^4} \quad [13]$$

More simply, [13] is equivalent to $\widehat{CV}^2(\hat{N}) = \widehat{CV}^2(\tilde{N}) + \widehat{CV}^2(\hat{p}_1(0))$.

RESULTS

2017 Eastern Bering Sea Beluga Aerial Line-transect Surveys

Between 16 and 29 June 2017, a total of 16 survey flights (62 flight hours) were conducted on 12 days. The survey flights covered a total of 15,340 km, including 8,587 km on transect. There was no sea ice observed during the 2017 surveys.

Belugas were observed from Shaktoolik to the southernmost transect, located approximately 50 km north of Scammon Bay (Fig. 1). All belugas were sighted within 120 km of the coast. The beluga distribution ranged farthest offshore near Unalakleet and was constrained closest to shore (within 40 km of the coast) from the Yukon River Delta to the southern boundary of the study area. In total, 1,897 belugas were sighted, resulting in an encounter rate (number of belugas sighted per km surveyed) of 0.221 belugas/km (Table 3). The beluga total for 2017 included 95 calves (as defined above); 2 beluga carcasses were also detected. Beluga group sizes during the 2017 surveys ranged from 1 to 39 whales; the stratum with the largest average group size (3.5 belugas per group) was located south of the Yukon Delta (Table 4). Belugas were sighted only

during transect effort; zero beluga sightings were made while on search and none were recorded during circling from transect. The plane broke from the transect to circle on only 12 occasions, in order to investigate and photograph marine mammal carcasses and confirm species identification of killer (*Orcinus orca*) and gray whale (*Eschrichtius robustus*) sightings.

The complete list of other marine mammals sighted during the 2017 survey includes 3 gray whales (including 1 calf), 6 killer whales (including 1 calf), 1 minke whale (*Balaenoptera acutorostrata*), 2 large whales (minke whale or larger) that could not be identified to species, 84 small pinnipeds, and 12 walrus carcasses (*Odobenus rosmarus divergens*).

ASAMM 2018 and 2019 Imagery

The photo analysts identified 225 beluga sightings in imagery that were matched to ASAMM aerial observer sightings, 44 beluga imagery sightings that were missed by ASAMM aerial observers, and 66 IR beluga sightings.

Multiple Covariates Distance Sampling Detection Function for the EBS Beluga Aerial Survey

The final hazard-rate detection function model for the EBS beluga aerial survey incorporated only one covariate, turbidity, suggesting that turbidity decreased the distance at which belugas were detected (Table 5). The detection function model with both turbidity and Beaufort Sea State had a lower AIC than the model with turbidity alone; however, the more complex model was within 2 AIC units of the model with only turbidity (Table 6), so we selected the simpler model for the abundance estimate (Burnham and Anderson 2002). The average unconditional detection probability for the turbidity model was 0.646, resulting in an effective strip half-width of 610 m.

For comparison, the effective strip half-width for the detection function model with both turbidity and Beaufort Sea State was 613 m, a negligible difference.

To evaluate the fit of the mcds model, we examined the histogram of perpendicular sighting distances overlaid with model fit (Fig. 4) and conducted a Cramer von Mises goodness-of-fit test (test statistic = 0.039, p = 0.937).

Mark-recapture Detection Functions for ASAMM

ASAMM aerial observers detected a total of 850 beluga sightings that were included in the mark-recapture detection function model. The best mark-recapture model incorporated a categorical group size variable (*catsizeGT2*, Tables 7 and 8) along with perpendicular sighting distance and indicated that transect detection probability was higher for larger groups. The estimates of $\hat{p}_1(0, \boldsymbol{z}_j)$ for IR-detected were 0.729 for single belugas, 0.863 for groups of two belugas, and 1.0 for groups with more than two belugas. The corresponding estimates of $\hat{p}_1(0, \boldsymbol{z}_j)$ for IR-missed were 0.578, 0.827, and 0.895; and for IR-omitted were 0.681, 0.861, and 1.0. The estimate of average transect detection probability, $\hat{p}_1(0)$, for IR-detected was 0.785 ($\widehat{CV}(\hat{p}_1(0))$ = 0.009); the corresponding values for IR-missed and IR-omitted were 0.648 ($\widehat{CV}(\hat{p}_1(0))$ = 0.200) and 0.753 ($\widehat{CV}(\hat{p}_1(0))$ = 0.015), respectively.

To evaluate model fit, we conducted chi-square goodness-of-fit tests: IR-detected chi-square = 5.564, p = 0.961 with 13 degrees of freedom; IR-missed chi-square = 6.850, p = 0.811 with 11 degrees of freedom; IR-omitted chi-square = 6.923, p = 0.805 with 11 degrees of freedom.

Based on expert judgment, we recommend using the transect detection probability estimate derived from the IR-omitted scenario (0.753) to estimate abundance of the EBS beluga stock in 2017.

Availability Probability

Our estimate of availability probability, $p^*_{a,avg}(0)$, was 0.499, resulting in an availability bias correction factor of 2.0. It is important to note that, because our analysis was limited to the summary statistics presented in Frost and Lowry (1995, their Table 1), our resulting estimate of $p^*_{a,avg}(0)$ is negatively biased. This is because we did not have the correct weights derived from the cutpoint of $T(0)$ = 15.9 sec, so we used the weights associated with $T(0)$ = 10.3 sec. For the scenario in which $T(0)$= 15.9, there would be more weight in $p^*_{a,k}(0)$ given to $p_a(0)$ = 1.0 than these results provide. As a result, $p^*_{a,avg}(0)$ would be higher and the associated correction factor would be lower.

Abundance and Uncertainty Estimates

To facilitate a direct comparison of results from the 2000 and 2017 EBS beluga aerial surveys, we first present estimates of abundance and density by stratum that have not been corrected for availability bias or transect detection probability. We refer to these estimates as "uncorrected" abundance and density estimates. For 2017, the uncorrected abundance estimates by stratum ranged from a low of 613 belugas off Yukon Delta to a high of 1,731 off Unalakleet (Table 4). The south Yukon Delta stratum had the highest overall density (0.329 belugas/km^2), followed by west/south Stuart Island (0.199 belugas/km^2), Yukon Delta (0.193 belugas/km^2), and west Unalakleet (0.107 belugas/km^2), respectively (Table 4). The total overall uncorrected abundance estimate for 2017 was 4,621 belugas (CV = 0.12).

Here, we present the results from the sensitivity analyses, which correspond to estimates of abundance and associated uncertainty that have been corrected for the best available estimates of availability bias and transect detection probability (Table 9). Using our estimated availability bias correction factor of 2.0, the corrected estimates of EBS beluga abundance in 2017 were: 11,768 belugas (CV = 0.117) for the IR-detected scenario; 14,243 belugas (CV = 0.231) for the IR-missed scenario; and 12,269 belugas (CV = 0.118) for the IR-omitted scenario, the scenario judged most likely by our expert panel.

DISCUSSION

We presented estimates of abundance for the EBS beluga stock in 2017 that were based on a conventional (geographically stratified) line-transect distance-sampling analysis that is comparable to the analytical methods that Lowry et al. (2017) used to estimate abundance for this stock in 2000. Additionally, we incorporated the best available information on transect detection probability and availability bias to reduce bias in the overall population abundance estimate. Although estimates of detection probability and availability bias are likely to become more accurate and precise based on future efforts to refine them, we have presented our results in a way that a revised abundance estimate can easily be computed using new correction factors in order to consistently estimate abundance and trend.

Compared to previous ABWC aerial surveys conducted in the Norton Sound/Yukon Delta region, the 2017 survey covered the most kilometers on transect, encompassed the largest survey area, and detected the highest number of belugas (Table 3). The beluga encounter rates for the ABWC aerial surveys conducted in June 1992 (0.223 belugas/km) and 1995 (0.257 belugas/km) were slightly higher than in 2017 (0.221 belugas/km) (Table 3). Although the beluga distribution in 2017 was similar to that observed during previous ABWC aerial surveys (Lowry et al. 2017),

there were some differences in estimated density and abundance among the four strata used in the analysis. The largest apparent increase in estimated stratum abundance occurred in the west Unalakleet and south Yukon strata, where the 2017 abundance estimates (uncorrected for transect detection probability) were 7.4 times and 7.3 times (respectively) greater than in 2000. In contrast, stratum abundances appeared lower in 2017 in the west/south Stuart Island and Yukon River strata, estimated to be only 0.7 and 0.5 times (respectively) the estimated abundances in 2000. These spatial differences in density and abundance may reflect interannual variability in seasonal chronology and differences in availability of salmon which are likely the major prey at this time of year. Alternatively, they may reflect sampling variability because belugas transit the region searching for prey, yet the aerial survey data reflect only a snapshot in time.

Without correcting for transect detection probability and using the same availability bias correction factor as Lowry et al. (2017), we estimated the total abundance of EBS belugas in 2017 to be 9,242 belugas (CV = 0.12) compared to 6,994 belugas (CV = 0.37) in 2000 (Lowry et al. 2017). The lower CV in the 2017 abundance estimate likely results from the ability to survey more transects in 2017 due to the longer field season and good weather. We recommend that future aerial surveys to estimate abundance of this stock are planned to occur over the same (or longer) survey duration as used in 2017 to maximize chances that weather will be conducive for surveying during the field period and to minimize uncertainty in the resulting abundance estimates.

After incorporating correction factors for transect detection probability, our sensitivity analyses suggest that the best estimate of abundance for EBS belugas in 2017 was between 11,768 and 14,243 belugas. Using expert judgment to select the most likely transect detection probability

estimate, the recommended estimate of EBS beluga abundance in 2017 is 12,269 belugas (CV = 0.118). The precision of the recommended abundance estimate is within the range (CV ≤ 0.3) that NOAA considers desirable for assessing marine mammal stocks (NMFS 2004). The abundance estimate for this stock can be further refined only with additional information about availability probability and transect detection probability, and the uncertainties associated with these probabilities.

Our availability bias correction factor was based on data from only three belugas for only a few hours (Frost and Lowry 1995), none of which were from the EBS stock. Furthermore, the correction factor that we derived was positively biased due to reliance on summary statistics that were derived for a different value of time-in view (Frost and Lowry 1995). To increase the accuracy and precision of the availability probability estimate, it may be feasible and cost-effective to collect data on beluga surface intervals and dive intervals using unmanned aerial systems (UAS). Because beluga surfacing and diving behavior varies with habitat, activity state, and possibly social structure of the group, these factors should be considered when designing studies to collect data to improve availability probability estimates and when evaluating the potential biases that may result from applying particular availability probability estimates to estimate population abundance.

To refine the transect detection probability estimate, including the effects of potentially important covariates such as turbidity and beluga size or coloration, additional aerial line-transect surveys that incorporate double observer methods (e.g., two teams of marine mammal observers, or one team of marine mammal observers plus synchronous collection of imagery on the transect) will be necessary. However, determining whether beluga sightings in the independent databases represent matches is a particularly difficult task for species like belugas

that tend to cluster on multiple spatial scales. In these scenarios, the sightings occur in quick succession and there is often no clear distinction among groups of animals (Hamilton et al. 2018).

Due to multiple confounding factors, we were unable to investigate whether survey altitude affected transect detection probability within the range of altitudes considered here. The EBS beluga surveys targeted an altitude of 320 m above sea level, whereas the ASAMM surveys that were used to estimate transect detection probability targeted 400 m above sea level. The former specifically targeted a lower altitude so that belugas would appear larger to the aerial observers. It is interesting to note that although the left-truncation distances used for the detection functions for each survey dataset differed, the corresponding declination angles were similar. At approximately 320 m survey altitude, a perpendicular sighting distance of ~50 m corresponds to a declination angle of approximately 81°. At ~ 400 m survey altitude, a perpendicular sighting distance of ~100 m corresponds to a declination angle of approximately 75°.

Estimating a correction factor to account for undetected newborns and yearlings in beluga abundance estimates derived from aerial surveys is a particularly difficult task. Brodie (1971) derived a correction factor for this source of bias based on an estimate of the proportion of the beluga population comprising these young age classes in Cumberland Sound during late August 1967. Brodie's (1971) method required assumptions about the proportion of the population that is female, female age of maturity, female calving interval, survival to the first year, and the proportion of newborns and yearlings that are dark. Additionally, Brodie (1971) estimated beluga age under the assumption that two growth layer groups (GLGs) are deposited per year in beluga teeth. However, recent studies concluded that only a single GLG is deposited each year (Hohn et al. 2016, Lockyer et al. 2016, Matthews and Ferguson 2014, Read et al. 2018, Waugh et al.

2018, Vos et al. 2020). Based on all of these assumptions, Brodie (1971) estimated that 15.2% of the belugas in the population were newborns or yearlings. Therefore, he proposed applying a correction factor of 1.18 to an abundance estimate derived from aerial survey data. We do not recommend this approach because it relies on a number of assumptions about population dynamics that are difficult to estimate and may vary across populations and over time, especially during periods of rapid ecological change, such as presently occurring in Arctic marine ecosystems. Rather, we propose that aerial imagery from UAS may be used to estimate the proportion of time that newborn calves swimming close to an adult are visible from the air, and that additional data be collected during manned aerial surveys to estimate the effects of animal size or coloration on the detection function. Our proposed approach recasts the issue in terms of conditional probability: For every small or dark beluga detected, how many were likely missed?

More information may be extracted from the available time series of ABWC and NOAA aerial line-transect survey data for the Norton Sound/Yukon Delta region. Specifically, it is likely that abundance estimates derived from spatially explicit models would result in more reliable estimates of uncertainty and less bias because spatial models explicitly account for spatial autocorrelation in the data (Johnson et al. 2010, Miller et al 2013, Hedley and Bravington 2014, Ferguson et al. 2022). We recommend that the EBS beluga aerial survey data for each survey year be analyzed using spatially explicit models to estimate abundance and associated uncertainty. Second, to derive an effective conservation and management plan for the EBS stock that would help ensure the health of the beluga population, the communities who rely on the belugas, and the eastern Bering Sea ecosystem as a whole, we recommend that the spatially explicit abundance estimates be used in an analysis to determine the optimal time between subsequent future aerial surveys.

ACKNOWLEDGMENTS

To begin, thank you to the ABWC and the beluga hunters for their dedicated partnership with NOAA Fisheries to better understand belugas in Alaska through continued research, and to effectively manage the stocks so that they will continue to be available to current and future generations. A huge thank you to the 2017 pilots, Sarah Corbin and Channing Wilson. It is physically and mentally challenging to survey as much as they did in such a short period of time, but they exceeded expectations in every way possible and they accomplished their task with a perfect safety record. Thanks, also, to the behind-the-scenes people at Clearwater Air who helped plan and stage the surveys: Andy Harcombe, Terika Kons, and Jake Turner. Thank you to the dispatchers at the Department of Interior (DOI), Bureau of Land Management, Alaska Interagency Coordination Center, South Zone Dispatch who vigilantly followed every flight and were ready to take necessary actions in the event of an emergency. We'd like to thank Doug DeMaster, John Bengtson, Phil Clapham, Robyn Angliss, and Nancy Friday, leadership at the Alaska Fisheries Science Center (AFSC) and the Marine Mammal Laboratory, who were instrumental in finding the financial support for this project and enabling us to take time away from other projects to devote to planning and conducting these surveys. Lloyd Lowry and Rod Hobbs participated in early planning sessions, and Lloyd graciously provided input throughout the entire project. The aircraft contracts were made possible through the assistance of the DOI Acquisition Services Directorate (Valerie Flynn, Vanessa Chavez, and Richard Davis), the North Slope Borough Department of Wildlife Management, and AFSC employees Stefan Ball, Mary Foote, and Ben Riedesel. Mike Hay of XeraGIS created the ASAMM Survey software, enabling accurate and precise data collection and rapid turnaround of summary statistics and maps in the flight reports. Lori Quakenbush and John Citta from the Alaska Department of Fish and Game

shared beluga tagging data. The University of Washington's Joint Institute for the Study of the Atmosphere and Ocean and Cooperative Institute for Climate, Ocean, and Ecosystem Studies helped us support the aerial survey observers, both in the field and at the lab. Thank you to Janet Clarke for teaching us how this is done and to Kim Shelden for the chocolate. We appreciate the technical reviews of earlier drafts of this analysis that were provided by Paul Conn, Paul Wade, Thomas Doniol-Valcroze, John Citta, and Kathy Frost. Finally, M. Ferguson would like to thank her canine wingman, Toby Ferguson, who was in his 10th season of aerial surveys in 2017, having mastered the art of flight following and data editing while chasing squirrels or balls, or patrolling the neighborhood. The survey was conducted under NMFS Permit No. 20465. The views expressed here are those of the authors and do not necessarily reflect the views of the U.S. National Marine Fisheries Service, NOAA.

CITATIONS

Adams, M., K. J. Frost, and L. Harwood. 1993. Alaska and Inuvialuit Beluga Whale Committee (AIBWC) - an initiative in "at home management". Arctic 46(2): 134–137.

Bivand, R., and N. Lewin-Koh. 2019. maptools: Tools for Reading and Handling Spatial Objects. R package version 0.9-9. Available from: https://CRAN.R-project.org/package=maptools.

Bivand, R., and C. Rundel. 2019. rgeos: Interface to Geometry Engine - Open Source ('GEOS'). R package version 0.5-2. Available from: https//CRAN.R-project.org/package=rgeos.

Bivand, R., T. Keitt, and B. Rowlingson. 2019. rgdal: Bindings for the 'Geospatial' Data Abstraction Library. R package version 1.4-8. Available from: https://CRAN.R-project.org/package=rgdal.

Bivand, R. S., E. J. Pebesma, and V. Gomez-Rubio. 2013. Applied Spatial Data Analysis with R, Second Edition. Springer, NY. Available from: http://www.asdar-book.org/.

Brodie, P. F. 1971. A reconsideration of aspects of growth, reproduction, and behavior of the white whale (*Delphinapterus leucas*), with reference to the Cumberland Sound, Baffin Island, population. J. Fish. Res. Bd. Can. 28: 1309-1318.

Buckland, S. T., D. R. Anderson, K. P, Burnham, J. L. Laake, D. L. Borchers, and L. Thomas. 2001. Introduction to Distance Sampling: Estimating Abundance of Biological Populations. Oxford University Press, Oxford. 432 p.

Burnham, K. P. and D. R. Anderson. 2002. Model Selection and Multimodel Inference: A Practical Information-Theoretic Approach. 2nd edition. Springer, New York. 488 p.

Burt, M. L., D. L. Borchers, K. J. Jenkins, and T. A. Marques. 2014. Using mark–recapture distance sampling methods on line transect surveys. Meth. Ecol. Evol. 5(11): 1180-1191. (doi: 10.1111/2041-210X.12294).

Citta, J. J., P. Richard, L. F. Lowry, G. O'Corry-Crowe, M. Marcoux, R. Suydam, L.T. Quakenbush, R. C. Hobbs, D. I. Litovka, K. J. Frost, T. Gray, J. Orr, B. Tinker, H. Aderman, and M. L. Druckenmiller. 2017. Satellite telemetry reveals population specific winter ranges of beluga whales in the Bering Sea. Mar. Mammal Sci. *33*(1): 236-250. (doi: 10.1111/mms.12357).

Clarke, J. T., A. A. Brower, M. C. Ferguson, and A. L. Willoughby. 2019. Distribution and relative abundance of marine mammals in the Eastern Chukchi and Western Beaufort Seas, 2018. Annual Report, OCS Study BOEM 2019-021. 451 p.

Clarke, J. T., A. A. Brower, M. C. Ferguson, A. L. Willoughby, and A. D. Rotrock. 2020. Distribution and relative abundance of marine mammals in the Eastern Chukchi Sea, Eastern and Western Beaufort Sea, and Amundsen Gulf, 2019. Annual Report, OCS Study BOEM 2020-027. 603 p.

Danovaro, R., E. Fanelli, J. Aguzzi, D. Billett, L. Carugati, C. Corinaldesi, A. Dell'Anno, K. Gjerde, A. J. Jamieson, S. Kark, C. McClain, L. Levin, N. Levin, E. Ramirez-Llodra, H. Ruhl, C. R. Smith, P. V. R. Snelgrove, L. Thomsen, C. L. Van Dover, and M. Yasuhara. 2020. Ecological variables for developing a global deep-ocean monitoring and conservation strategy. Nat. Ecol. Evol. 4: 181–192. (doi: 10.1038/s41559-019-1091-z).

Ferguson, M. C., J. T. Clarke, A. L. Willoughby, A. A. Brower, and A. D. Rotrock. 2021. Geographically stratified abundance estimate for Bering-Chukchi-Beaufort Seas bowhead whales (*Balaena mysticetus*) from an August 2019 aerial line-transect survey in the Beaufort Sea and Amundsen Gulf. U.S. Dep. Commer., NOAA Tech. Memo. NMFS-AFSC-428, 54 p.

Ferguson, M. C., D. L. Miller, J. T. Clarke, A. A. Brower, A. L. Willoughby, and A. D. Rotrock. 2022. Spatial modeling, parameter uncertainty, and precision of density estimates from line-transect surveys: a case study with Western Arctic bowhead whales. Paper SC/68d/ASI/01 presented to the IWC Scientific Committee, May 2022.

Fewster, R. M., S. T. Buckland, K. P. Burnham, D. L. Borchers, P. E. Jupp, J. L. Laake, and L. Thomas. 2009. Estimating the encounter rate variance in distance sampling. Biometrics 65(1): 225-236. (doi: 10.1111/j.1541-0420.2008.01018.x).

Frost, K. J., and L. F. Lowry. 1995. Radiotag based correction factors for use in beluga whale population estimation. Working paper for Alaska Beluga Whale Committee Scientific Workshop, Anchorage, AK, 5-7 April 1995.

Frost, K. J., L. F. Lowry, and R. R. Nelson. 1985. Radiotagging studies of beluga whales (Delphinapterus leucas) in Bristol Bay, Alaska. Mar. Mammal Sci. 1: 191-202.

Hain, J. H. W., S. L. Ellis, R. D. Kenney, and C. K. Slay. 1999. Sightability of right whales in coastal waters of the southeastern United States with implications for the aerial monitoring program, p. 191-208. *In*: G. W. Garner, S. C. Amstrup, J. L. Laake, B. F. J. Manly, L. L. McDonald, and D. G. Robertson (eds.), Marine Mammal Survey and Assessment Methods A. A. Balkema, Rotterdam.

Hamilton, O. N. P., S. E. Kincaid, R. Constantine, L. Kozmian-Ledward, C. G. Walker, and R. Fewster. 2018. Accounting for uncertainty in duplicate identification and group size judgements in mark–recapture distance sampling. Meth. Ecol. Evol. 9: 354– 362. (doi: 10.1111/2041-210X.12895).

Hedley, S. and M. Bravington. 2014. Comments on design-based and model-based abundance estimates for the RMP and other contexts. Paper SC/65B/RMP/11 presented to the IWC Scientific Committee, May 2014.

Hohn, A. A., C. Lockyer, and M. Acquarone. 2016. Report of the workshop on age estimation in monodontids. Tampa, FL, 26–November 27, 2011. NAMMCO Sci. Publ. No. 10. (doi: 10.7557/3.3743).

Huntington, H. P., and the communities of Buckland, Elim, Koyuk, Point Lay, and Shaktoolik. 1999. Traditional knowledge on the ecology of beluga whales (*Delphinapterus leucas*) in the eastern Chukchi and northern Bering Seas, Alaska. Arctic. 52:1: 49-61.

Johnson, D. S., J. L. Laake, and J. M. Ver Hoef. 2010. A model-based approach for making ecological inference from distance sampling data. Biometrics 66(1): 310-318. (doi: 10.1111/j.1541-0420.2009.01265.x).

Laake, J. L., and D. L. Borchers. 2004. Methods for incomplete detection at distance zero, p. 109-189. *In*: S. T. Buckland, D.R. Anderson, K.P. Burnham, J.L. Laake, D.L. Borchers, and L. Thomas (Editors), Advanced Distance Sampling: Estimating Abundance of Biological Populations. Oxford University Press, Oxford.

Laake, J., D. Borchers, L. Thomas, D. Miller, and J. Bishop. 2021. mrds: Mark-Recapture Distance Sampling. R package version 2.2.5.9003. Available from: https://github.com/DistanceDevelopment/mrds/.

Lettrich, M. D., D. M. Dick, C. C. Fahy, R. B. Griffis, H. L Haas, T. T. Jones, I. K. Kelly, D. Klemm, A. M. Lauritsen, C. R. Sasso, B. Schroeder, J. A. Seminoff, and C. M. Upite. 2020. A method for assessing the vulnerability of sea turtles to a changing climate. U.S. Dep. Commer., NOAA Tech. Memo. NMFS-F/SPO-211, 84 p.

Lockyer, C., A.A. Hohn, R. Hobbs, and R.E.A. Stewart. 2016. Report on the workshop on age estimation in beluga. Beaufort, NC, 5–December 9, 2011. NAMMCO Sci. Publ. No. 10. (doi: 10.7557/3.3731).

Lowry, L. F., J. J. Citta, G. O'Corry-Crowe, L. T. Quakenbush, K. J. Frost, R. Suydam, R .C. Hobbs, and T. Gray. 2019. Distribution, abundance, harvest, and status of western Alaska beluga whale, *Delphinapterus leucas*, stocks. Mar. Fish. Rev. 81(3-4): 54-71. (doi: 10.7755/MFR.81.3–4.2).

Lowry, L. F., A. Zerbini, K. J. Frost, D. P. DeMaster, and R. C. Hobbs. 2017. Development of an abundance estimate for the eastern Bering Sea stock of beluga whales (*Delphinapterus leucas*). J. Cetacean Res. Manage. 16: 39-47.

Marsh, H. and D. Sinclair. 1989. Correcting for visibility bias in strip transect aerial surveys of aquatic fauna. J. Wild. Manage. 53(4): 1017–1024. (doi: 10.2307/3809604).

Marques, F. F. C., and S. T. Buckland. 2003. Incorporating covariates into standard line transect analyses. Biometrics 59: 924-935. (doi: 10.1111/j.0006-341X.2003.00107.x).

Matthews, C. J. D., and S. H. Ferguson. 2014. Validation of dentine deposition rates in beluga whales by interspecies cross dating of temporal $\delta^{13}C$ trends in teeth. NAMMCO Sci. Publ. No. 10. (doi: 10.7557/3.3196).

McLaren, I. A. 1961. Methods of determining the numbers and availability of ringed seals in the eastern Canadian Arctic. Arctic 14: 162-175.

Miller, D. L., M. L. Burt, E. A. Rexstad, and L. Thomas. 2013. Spatial models for distance sampling data: recent developments and future directions. Meth. Ecol. Evol. 4: 1001–1010. (doi: 10.1111/2041-210X.12105).

National Marine Fisheries Service (NMFS). 2004. A requirements plan for improving the understanding of the status of U.S. protected marine species: report of the NOAA Fisheries National Task Force for Improving Marine Mammal and Turtle Stock Assessments. 112 p. Available from: https://repository.library.noaa.gov/view/noaa/3421. Accessed December 2022.

Oceana and Kawerak Inc. (2014). The Bering Strait marine life and subsistence use data synthesis. Kawerak Incorporated. 499 p. Available from: https://oceana.org/publications/reports/the-bering-strait-marine-life-and-subsistence-data-synthesis.

O'Corry-Crowe, G., T. Ferrer, J.J. Citta, R. Suydam, L. Quakenbush, J.J. Burns, J. Monroy, A. Whiting, G. Seaman, W. Goodwin, Sr., M. Meyer, S. Rodgers, and K.J. Frost. 2021. Genetic history and stock identity of beluga whales in Kotzebue Sound. Polar Res. 40: 7623. (doi: 10.33265/polar.v40.7623).

O'Corry-Crowe, G., R. Suydam, L. Quakenbush, B. Potgieter, L. Harwood, D. Litovka, T. Ferrer, J. Citta, V. Burkanov, K. Frost, and B. Mahoney. 2018. Migratory culture, population structure and stock identity in North Pacific beluga whales (*Delphinapterus leucas*). PLoS ONE 13(3): e0194201. (doi: 10.1371/journal.pone.0194201).

Pebesma, E. J. and R. S. Bivand. 2005. Classes and methods for spatial data in R. R News 5 (2). Available from: http://cran.r-project.org/doc/Rnews/.

R Core Team. 2021. R: A language and environment for statistical computing. R Foundation for Statistical Computing, Vienna, Austria. URL https://www.R-project.org/.

Read, F. L., A. A. Hohn, and C. H. Lockyer. 2018. A review of age estimation methods in marine mammals with special reference to monodontids. NAMMCO Sci. Publ. No. 10. (doi: 10.7557/3.4474).

Vos, D. J., K. E. W. Shelden, N. A. Friday, and B. A. Mahoney. 2020. Age and growth analyses for the endangered belugas in Cook Inlet, Alaska. Mar. Mammal Sci. 36: 293-304. (doi: 10.1111/mms.12630)

Waugh, D. A., R. S. Suydam, J. D. Ortiz, and J. G. M. Thewissen. 2018. Validation of Growth Layer Group (GLG) depositional rate using daily incremental growth lines in the dentin of beluga (*Delphinapterus leucas* [Pallas, 1776]) teeth. PLoS ONE 13(1): e0190498. (doi: 10.1371/journal.pone.0190498).

Willoughby, A., M. Ferguson, B. Hou, C. Accardo, A. Rotrock, A. Brower, J. Clarke, S. Hanlan, M. Foster Doremus, K. Pagan, and L. Barry. 2021. Belly port camera imagery collected to address cetacean perception bias during aerial line-transect surveys: Methods and sighting summaries. U.S. Dep. Commer., NOAA Tech. Memo. NMFS-AFSC-427, 111 p.

Wood, S. N. 2017. Generalized Additive Models: An Introduction with R (2nd edition). Chapman and Hall/CRC. 496 p.

Table 1. -- Definitions of covariates considered for inclusion in the multiple covariates distance sampling detection function models for the 2017 eastern Bering Sea beluga line-transect aerial survey.

Covariate name	Definition	Categories
size	Observed group size of the sighting	
loggs	$\log_{10}(size)$	
catsize	Categorical group size	{1, >1}
catsizeGT2	Categorical group size	{1, 2, >2}
iBeauf	Integer-valued Beaufort Sea State	
Turb	Turbidity	yes, no

Table 2. -- Definitions of covariates considered for inclusion in the mark-recapture detection function models for the Aerial Surveys of Arctic Marine Mammals data.

Covariate name	Definition	Categories
loggs	ln(*size*)	
catsize	Categorical group size	{1, >1}
catsizeGT2	Categorical group size	{1, 2, >2}
iBeauf	Integer-valued Beaufort Sea State	
f4Beauf	Categorical Beaufort Sea State	{0 to 2; 3 to 4}

Table 3. -- Summary statistics from the Alaska Beluga Whale Committee and NOAA aerial surveys for belugas conducted in the Norton Sound/Yukon Delta region between 1992 and 2017.

Survey dates	Transect effort (km)	Belugas counted	Encounter rate (belugas/km)	Study area (km^2)
17-21 June 1992	7,278	1,625	0.223	6,145
14-18 June 1993	5,539	374	0.068	10,975
11-16 June 1994	5,746	370	0.064	13,965
5-8 June 1995	4,450	750	0.169	19,983
20-22 June 1995	1,776	456	0.257	3,352
15-17 June 1999	3,366	589	0.175	15,794
17-20 June 2000	4,226	428	0.101	38,104
16-29 June 2017*	8,587	1,897	0.221	41,416

*Total area surveyed. Only effort and sightings in strata 1 through 4 were used to estimate abundance.

Table 4. -- Comparison of line-transect statistics, abundance (N) estimates, and associated coefficients of variation (CV(N)) for the Alaska Beluga Whale Committee and NOAA aerial surveys conducted in the Norton Sound/Yukon Delta region during 2000 (Lowry et al. 2017) and 2017. The density and abundance estimates provided in this table are referred to as "uncorrected" because they have not been corrected for availability or transect detection probability.

		2000		2017	
		N	CV(N)	N	CV(N)
Stratum 1: West Unalakleet (16,134 km^2)	Encounter rate	0.014	0.79	0.141	0.23
	Mean group size	1.040	0.04	1.600	
	Uncorrected density (individuals/km^2)	0.015	0.79	0.107	0.24
	Uncorrected abundance	233	0.79	1731	0.24
Stratum 2: West and South Stuart Island (6,896 km^2)	Encounter rate	0.181	0.58	0.241	0.15
	Mean group size	1.520	0.11	1.939	
	Uncorrected density (individuals/km^2)	0.280	0.60	0.199	0.15
	Uncorrected abundance	1,933	0.60	1376	0.15
Stratum 3: Yukon Delta (3,172 km^2)	Encounter rate	0.191	0.38	0.206	0.29
	Mean group size	1.950	0.09	2.943	
	Uncorrected density (individuals/km^2)	0.380	0.40	0.193	0.30
	Uncorrected abundance	1,206	0.40	613	0.30
Stratum 4: South of Yukon Delta (2,743 km^2)	Encounter rate	0.038	1.03	0.337	0.13
	Mean group size	1.180	0.10	3.482	
	Uncorrected density (individuals/km^2)	0.045	1.03	0.329	0.15
	Uncorrected abundance	124	1.03	902	0.15
TOTAL (28,946 km^2)	Uncorrected density (individuals/km^2)	0.121	0.37	0.160	0.12
	Uncorrected abundance	3,497	0.37	4621	0.12

Table 5. -- Parameter estimates for the final multiple covariates distance sampling detection function model with the hazard-rate key function. The model was constructed from the data collected during the Alaska Beluga Whale Committee and NOAA 2017 Norton Sound/Yukon Delta line-transect aerial survey on the Turbo Commander aircraft.

		Estimate	Standard Error
Scale Coefficients	*Intercept*	-0.611	0.077
	Turb - yes	-0.346	0.117
Shape Coefficients			
	Intercept	0.859	0.149

Table 6. -- Model evaluation statistics for the multiple covariates distance sampling detection function models fit to the 2017 eastern Bering Sea beluga aerial line-transect survey data.

Model covariates	AIC	ΔAIC	AIC Weight	Log-likelihood
Turbidity + iBeauf	-217.41	0.00	0.34	112.71
Turbidity	-217.32	0.09	0.32	111.66
Turbidity + catsize	-216.99	0.42	0.27	112.49
iBeauf	-211.31	6.10	0.02	108.65
catsize	-211.23	6.18	0.02	108.61
catsizGT23	-211.08	6.33	0.01	109.54
null model	-210.66	6.75	0.01	107.33
loggs	-209.17	8.24	0.01	107.59
size	-208.70	8.71	0.00	107.35

Table 7. -- Parameter estimates for the final mark-recapture detection function models for the Aerial Surveys of Arctic Marine Mammals 2018-2019 beluga data based on aerial observer and imagery sightings. IR = inconclusive results.

		Estimate	Standard Error
IR-detected	*Intercept*	0.99	0.30
	distance	6.33	2.57
	catsizeGT2 (2)	0.86	0.50
	catsizeGT2 (>2)	16.85	1154.15
IR-missed	*Intercept*	0.31	0.24
	distance	0.77	1.77
	catsizeGT2 (2)	1.25	0.37
	catsizeGT2 (>2)	1.82	0.62
IR-omitted	*Intercept*	0.76	0.31
	distance	5.44	2.62
	catsizeGT2 (2)	1.06	0.51
	catsizeGT2 (>2)	17.17	1217.06

Table 8. -- Model evaluation statistics and resulting average transect detection probability estimates, $\hat{p}_1(0)$, for the mark-recapture distance sampling detection function models fit to the Aerial Surveys of Arctic Marine Mammals aerial line-transect survey and imagery data.

Model covariates	AIC	ΔAIC	AIC Weight	Log-likelihood	$\hat{p}_1(0)$
catsizeGT2	250.05	0.00	0.41	-121.02	0.785
catsize	251.87	1.82	0.16	-122.93	0.778
loggs	257.49	7.44	0.01	-125.75	0.780
null model	258.18	8.14	0.01	-127.09	0.778
f4Beauf	259.31	9.26	0.00	-126.65	0.775
iBeauf	259.72	9.67	0.00	-126.86	0.781

Table 9. -- Estimated abundance (N) and associated estimated coefficients of variation (CV(N)) of eastern Bering Sea belugas in 2017 for each combination of the three analytical methods to address imagery sightings with inconclusive results (IR) during manual matching. Uncertainty estimates do not exist for the availability bias correction factors, so the estimated coefficients of variation in abundance depended only on the IR scenarios.

	IR-detected	IR-missed	IR-omitted
N	11,768	14,243	12,269
CV(N)	0.117	0.231	0.118

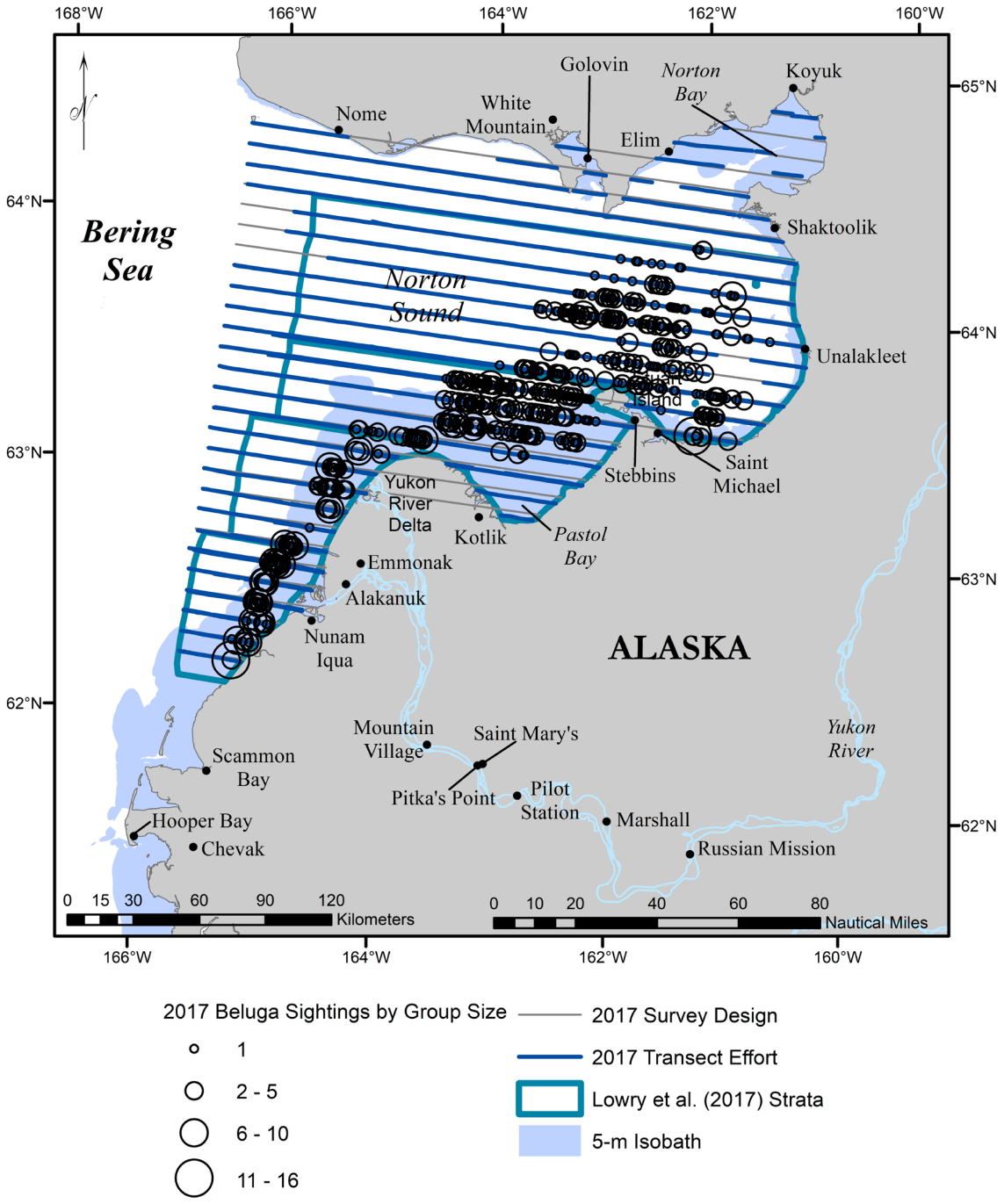

Figure 1. -- 2017 Eastern Bering Sea beluga aerial line-transect survey study area and survey design. Beluga sightings and transects flown during Beaufort Sea State ≤ 4 are shown. Waters shallower than 5 m are shaded, and the outlines of the geographic strata defined in Lowry et al. (2017) and used in the present analysis are shown in teal.

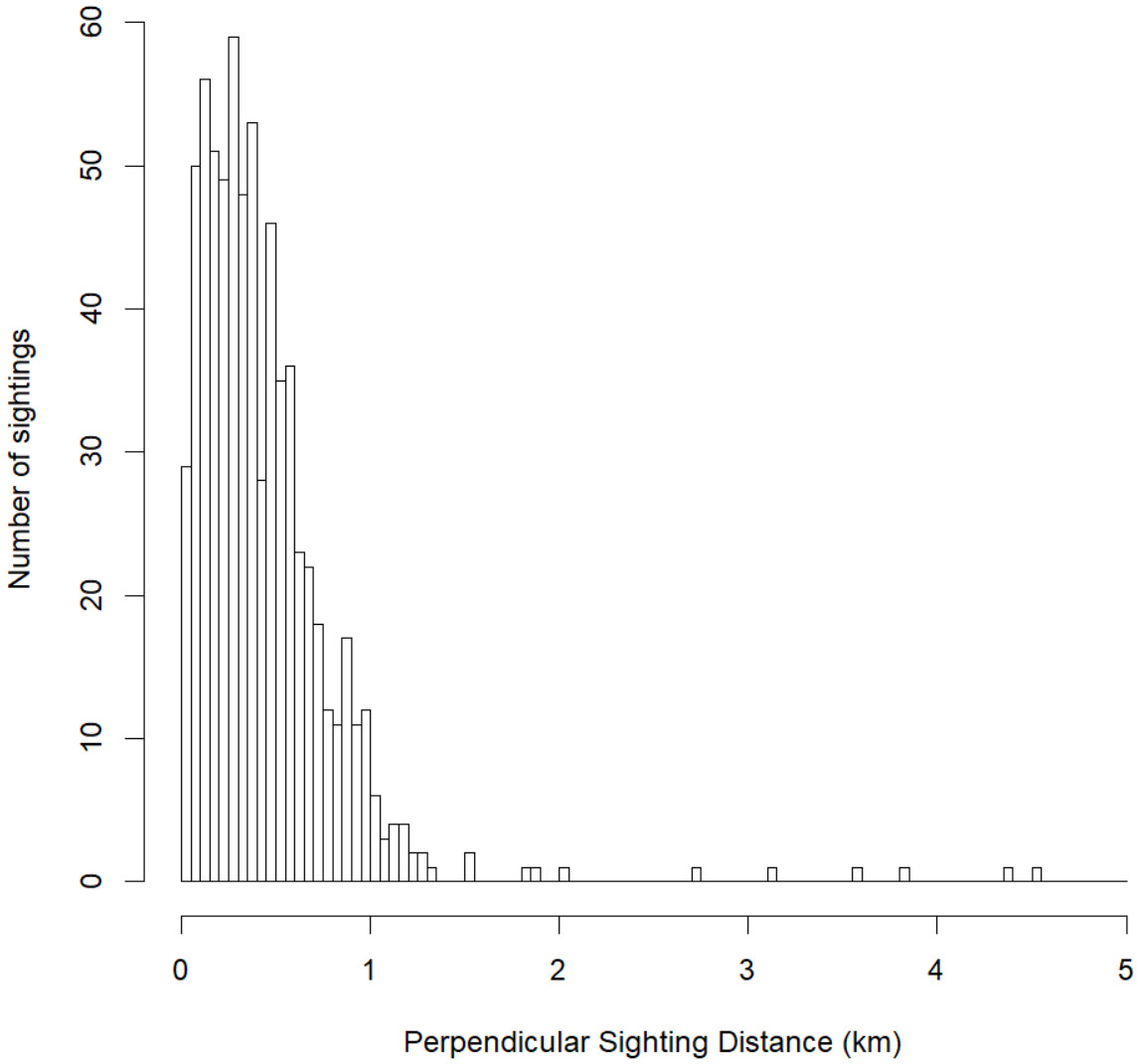

Figure 2. -- Perpendicular distances to beluga sightings during the 2017 Eastern Bering Sea beluga aerial line-transect survey.

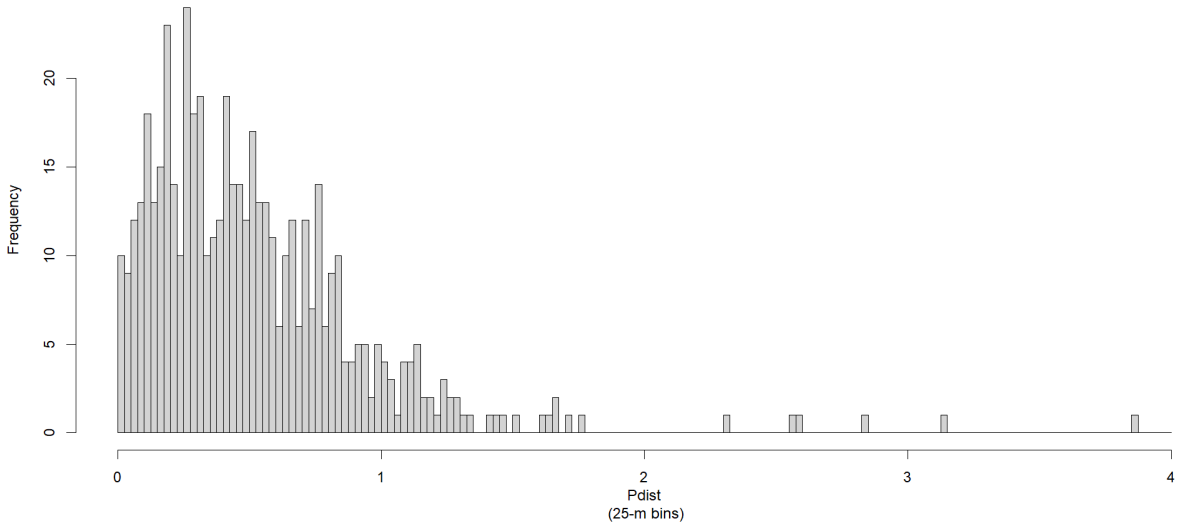

Figure 3. -- Perpendicular distances to beluga sightings during the 2018 and 2019 Aerial Surveys of Arctic Marine Mammals line-transect survey flights used in the mark-recapture distance sampling detection function.

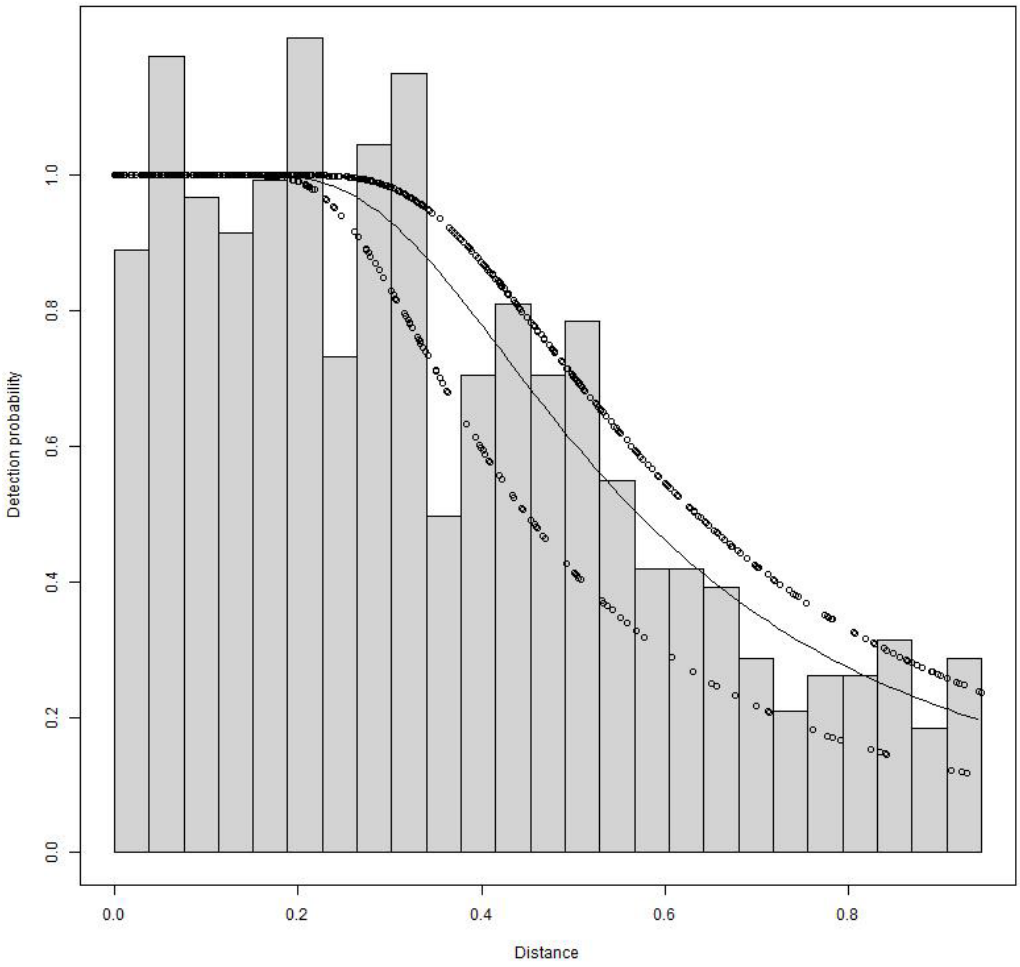

Figure 4. -- Histogram of perpendicular distances to beluga sightings and the multiple covariates distance sampling detection function model fit for the 2017 Eastern Bering Sea beluga aerial line-transect survey.

U.S. Secretary of Commerce
Gina M. Raimondo

Under Secretary of Commerce for Oceans and Atmosphere
Dr. Richard W. Spinrad

Assistant Administrator, National Marine Fisheries Service
Janet Coit

July 2023

www.nmfs.noaa.gov

OFFICIAL BUSINESS

National Marine Fisheries Service
Alaska Fisheries Science Center
7600 Sand Point Way N.E.
Seattle, WA 98115-6349